Induction of small cell lung cancer by somatic inactivation of both *Trp53* and *Rb1* in a conditional mouse model

Ralph Meuwissen,[1] Sabine C. Linn,[2] R. Ilona Linnoila,[4] John Zevenhoven,[1] Wolter J. Mooi,[3] and Anton Berns[1,*]

[1]Division of Molecular Genetics and Center of Biomedical Genetics, The Netherlands Cancer Institute, 1066 CX Amsterdam, The Netherlands
[2]Division of Medical Oncology
[3]Division of Pathology
The Netherlands Cancer Institute/Antoni van Leeuwenhoek Hospital, 1066 CX Amsterdam, The Netherlands
[4]Cell and Cancer Biology Department, Center for Cancer Research, National Cancer Institute, National Institute of Health, 9610 Medical Center Drive, Suite 300, Rockville, Maryland 20850
*Correspondence: a.berns@nki.nl

Summary

Small cell lung cancer (SCLC) is a highly aggressive human tumor with a more than 95% mortality rate. Its ontogeny and molecular pathogenesis remains poorly understood. We established a mouse model for neuroendocrine (NE) lung tumors by conditional inactivation of *Rb1* and *Trp53* in mouse lung epithelial cells. Mice carrying conditional alleles for both *Rb1* and *Trp53* developed with high incidence aggressive lung tumors with striking morphologic and immunophenotypic similarities to SCLC. Most of these tumors, which we designate MSCLC (murine small cell lung carcinoma), diffusely spread through the lung and gave rise to extrapulmonary metastases. In our model, inactivation of both Rb1 and p53 was a prerequisite for the pathogenesis of SCLC.

Introduction

Lung carcinoma is currently the most frequent cause of cancer deaths (Tyczynski et al., 2003; Minna et al., 2002). Clinically and histopathologically, lung carcinomas are divided into two major groups. Small cell lung carcinoma (SCLC), a highly malignant tumor of primitive neuroendocrine (NE) cells, is thought to arise from cells residing in the epithelial lining of the bronchi which share the NE phenotype (Wistuba et al., 2001). SCLC accounts for about 20% of all lung cancers, while the other, more heterogenous group of non-small cell lung cancers (NSCLC) accounts for 80%. SCLCs express markers of NE differentiation, whereas most NSCLCs lack these properties (Rom et al., 2000). SCLC metastasizes early and widely, accounting for the extremely poor prognosis of this tumor (Junker et al., 2000). Whereas SCLC often initially responds well to chemotherapy, relapses occur almost without exception, and they are usually resistant to cytotoxic treatment (Sandler, 2003). No unequivocal preneoplastic lesions have been associated with SCLC (Wistuba et al., 2001). Mutations commonly found during the pathogenesis of lung cancer are inactivation of *Rb1* and *Trp53*; indeed, these are identified in up to 90% of SCLCs (Gouyer et al., 1998; Sekido et al., 2003). Together with retinoblastoma, SCLC is the only human neural/neuroendocrine tumor that harbors *RB1* mutations in almost all cases (Sherr and McCormick, 2002). Chimeric mice from $Rb1^{-/-}$ ES cells and $Rb1^{+/-}$ mice developed extrapulmonary NE tumors but no apparent lung lesions (Jacks et al., 1992; Maandag et al., 1994). On the other hand $Rb1^{+/-};Trp53^{-/-}$ mice used in previous studies developed a variety of primary tumors of NE origin as well as focal bronchial NE cell hyperplasia, though they failed to develop NE lung tumors (Williams et al., 1994).

To study the role of Rb1 and p53 in the development of SCLC, we used the Cre-*loxP* system to obtain lung epithelium-specific deletion of *Rb1* and *Trp53* genes. Lungs of mice carrying conditional *Rb1* and *Trp53* alleles (Vooijs et al., 1998; Jonkers et al., 2001) were infected with Adeno-Cre (Ad-Cre) virus via intratracheal injection (Meuwissen et al., 2001). Somatic inactivation of both *Rb1* and *Trp53* alleles in a range of proliferating airway epithelial and alveolar type II cells lead to the development of multiple tumors with histopathology and immunophenotype closely mirroring human SCLC. These tumors diffusely invaded the surrounding lung parenchyma and readily metasta-

SIGNIFICANCE

Small cell lung cancer (SCLC) is a devastating lethal disease for which no cure is available. This study shows that concomitant loss of Rb and P53 in mouse lung causes a high incidence of SCLC recapitulating the salient features of human SCLC. The fact that loss of Rb and p53 in a broad range of epithelial cells gives rise almost exclusively to SCLC suggests that only a subset of cells are susceptible to transformation by these oncogenic events. These observations open the way to define the target cells and identify the signaling pathways crucial for SCLC. Furthermore, the high penetrance of murine SCLC will facilitate designing and testing of new treatment modalities against SCLC.

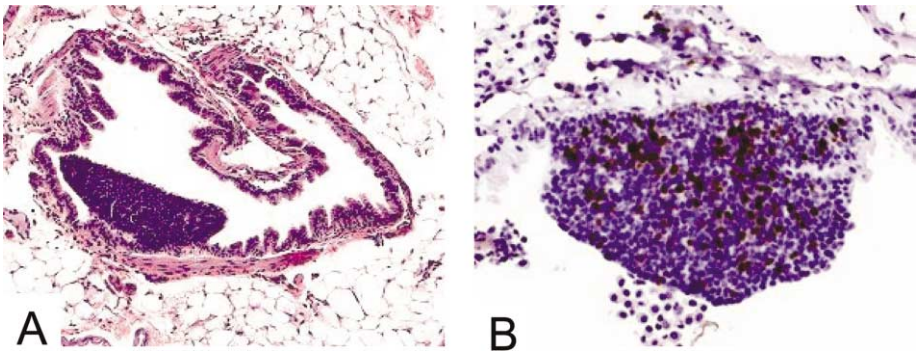

Figure 1. Photomicrographs of pulmonary NE epithelial hyperplasia in *Trp53*$^{F2\text{-}10/F2\text{-}10}$/*Rb1*$^{F19/F19}$ mice

A: A hyperplastic focus in the airway 2 months after Ad Cre revealing marked histologic dysplasia (H&E stain).

B: Extensive proliferation in a bronchial hyperplastic lesion indicated by anti-Brdu staining (immunoperoxidase stain).

sized to extrapulmonary sites, again very similar to human SCLC.

This tumor, which we designate murine small cell lung carcinoma (MSCLC), constitutes a murine SCLC tumor model. In view of the striking similarities to human SCLC, it is hoped that the model will be of value for the testing of chemoprevention and therapeutic strategies in SCLC.

Results

Somatic inactivation of *Rb1* and *Trp53* in lung epithelial cells leads to NE neoplastic lesions

In the light of the frequent inactivation of both *Trp53* and *Rb1* in various lung cancers, most notably in human SCLC, mice carrying conditional alleles for *Rb1* (floxed exon 19) and *Trp53* (floxed exons 2–10) were used (Vooijs et al., 1998; Jonkers et al., 2001). We administered Ad-Cre virus via either intratracheal injection or intubation (Meuwissen et al., 2001) in order to test whether the somatic inactivation of *Trp53* and *Rb1* in pulmonary epithelial cells can cause neoplasia with features of SCLC. Histologic examination of lungs from mice, sacrificed 6–8 weeks after Ad-Cre administration, showed the occurrence of multiple dysplastic foci of clustering small cells in the bronchial and bronchiolar mucosa in every animal tested (Figure 1A and Table 1). BrdU labeling indicated a high mitotic index within these lesions (Figure 1B), and immunostaining revealed positivity for synaptophysin (Syp) and the neural cell adhesion molecule Ncam1 (CD 56), indicating NE differentiation (Ferrari et al., 1999; Cavallaro et al., 2001).

These results are in accordance with earlier observations in lungs of 6-month-old *Trp53*$^{-/-}$;*Rb1*$^{+/-}$ mice (Williams et al., 1994), which also showed NE lesions in the airways. Interestingly, these lesions invariably showed loss of the wild-type Rb1 allele (Williams et al., 1994). In our case, PCR analysis for *Rb1* and *Trp53* recombination in microdissected specimens showed that both *Trp53* and *Rb1* alleles were inactivated in 4 out of 4 lesions investigated (results not shown). Apart from the focal NE proliferations, no other lesions were observed (Table 1), although Ad-Cre virus infection almost certainly will have inactivated both *Trp53* and *Rb1* in a broad range of different lung epithelial cells (Meuwissen et al., 2001). However, no obvious effect on Clara cell or alveolar type II cell proliferation was seen.

High incidence of metastasizing NE lung tumors from somatic mutation of *p53* and *Rb1*

Ad-Cre-treated *Trp53*$^{F2\text{-}10/F2\text{-}10}$;*Rb1*$^{F19/F19}$, *Trp53*$^{F2\text{-}10/+}$;*Rb1*$^{F19/F19,}$ and *Trp53*$^{F2\text{-}10/F2\text{-}10}$;*Rb1*$^{F19/+}$ mice were sacrificed when they became moribund. Most of the *Trp53*$^{F2\text{-}10/F2\text{-}10}$;*Rb1*$^{F19/F19}$ mice (Table 1) developed multiple independent tumors with a median latency of 210 days (Figure 2). Tumor onset and progression in these mice was relatively uniform, with tumors becoming detectable between 196 and 350 days. However, the median tumor-free survival of *Trp53*$^{F2\text{-}10/+}$;*Rb1*$^{F19/F19}$ and *Trp53*$^{F2\text{-}10/F2\text{-}10}$;*Rb1*$^{F19/+}$ mice was significantly longer, at 364 and 475 days, respectively. This demonstrates that combined loss of function of Rb1 and Trp53 contributes to lung tumorigenesis in these mice. Moreover, lung tumors were found in mice with all three genotypes, of which the majority (27/33) of *Trp53*$^{F2\text{-}10/F2\text{-}10}$;*Rb1*$^{F19/F19}$ mice showed almost exclusively SCLC-like tumors, whereas *Trp53*$^{F2\text{-}10/+}$;*Rb1*$^{F19/F19}$ and *Trp53*$^{F2\text{-}10/F2\text{-}10}$;*Rb1*$^{F19/+}$ mice often exhibited pulmonary adenocarcinomas as well as SCLCs (Table 1). We did not observe lung tumors in control *Rb1*$^{F19/F19}$ mice and only lung adenocarcinomas in *Trp53*$^{F2\text{-}10/F2\text{-}10}$ mice (Table 1). The *Rb1*$^{F19/F19}$ mice were monitored for up to 600 days before they were sacrificed. Histologic analysis of the lungs of *Trp53*$^{F2\text{-}10/F2\text{-}10}$;*Rb1*$^{F19/F19}$, *Trp53*$^{F2\text{-}10/+}$;*Rb1*$^{F19/F19}$ and *Trp53*$^{F2\text{-}10/F2\text{-}10}$;*Rb1*$^{F19/+}$ mice revealed tumors that were strikingly similar to human SCLC (Junker et al., 2000) (Figure 3). The cells of these tumors, which we designate murine small cell lung carcinomas (MSCLC) were small and featured densely hyperchromatic nuclei with a diffuse chromatin pattern that obscured the nucleolus (Figure 3N). Cytoplasm was poorly developed, and nuclear molding was commonly present (Figure 3N). The tumors grew mostly in sheets and generally spread massively and diffusely through the pulmonary tissues and air spaces, eliciting no or hardly any stromal response (shown in Figures 3B and 3M). There was high mitotic activity, with local fields of necrosis, and pronounced angioinvasion was present in some of the larger tumors. The MSCLCs lacked the typical glandular and tubular features of mouse adenocarcinomas. In a few mice (2/33), adenocarcinomas were however also identified, in addition to the MSCLCs. Several mice (6/33) developed medullary thyroid carcinomas, which had probably been induced by inadvertent spreading of Ad-Cre virus into the thyroid gland from the intratracheal injection site. Interestingly, the MSCLCs arising in *Trp53*$^{F2\text{-}10/F2\text{-}10}$;*Rb1*$^{F19/F19}$ mice (14/33) metastasized to a range of extrapulmonary sites, such as the bone, brain, adrenal gland, ovary, and liver (Figures 3G–3K, respectively). Like the primary tumors (Figure 3D), the metastases expressed thyroid transcription factor 1 (TITF1-1) (Ordonez, 2000; Wu et al., 2003), and their morphological appearance was identical to that of the primary lung tumors. In contrast, only a few metastases were associated with the small cell lung tumors from *Trp53*$^{F2\text{-}10/F2\text{-}10}$;*Rb1*$^{F19/+}$ (2/6), and none were found in *Trp53*$^{F2\text{-}10/+}$;

Table 1. Occurrence of lung tumors in conditional mutant mice

Genotype	Total number of mice	# of mice sacrificed with described pathology/# of mice analyzed	Histopathology of lung lesions	Lesion latency in days
$Rb^{F19/F19}$	8	0/8[a]	No lesions, normal	
$p53^{F2\text{-}10/F2\text{-}10}$	7	1/7[a]	Alveolar adenomatous hyperplasia	140d
		6/7[b]	Adenocarcinomas	350–530d
$p53^{F2\text{-}10/\Delta}$	6	6/6[b]	Adenocarcinomas	360–490d
$Rb^{F19/F19};p53^{F2\text{-}10/+}$	13	5/13[b]	Large SCLCs with sporadic adenocarcinomas	308-497d
		2/13[b]	Only medullary thyroid carcinomas	322–350d
		1/13[b]	Only adenocarcinomas	588d
		5/13[b]	No lesions	71–280d
$Rb^{F19/+};p53^{F2\text{-}10/F2\text{-}10}$	11	3/13[b]	Small SCLCs	392–584d
		1/13[b]	Small SCLCs and single adenocarcinomas	455d
		1/13[b]	Small SCLCs and metastases in mediastinum and ovary	520d
		1/13[b]	Small SCLCs and metastasis in adrenal gland	400d
		1/13[b]	Only adenocarcinomas	331d
		6/13[b]	No lesions	45–203d
$Rb^{F19/F19};p53^{F2\text{-}10/F2\text{-}10}$	4[a]	3/4	NE hyperplasia	(56–84d)
		1/4	No lesions	
	7[a]	5/7	NE hyperplasia and NE bronchial dysplasia	(105–175d)
		1/7	NE bronchial dysplasia and metastases in mediastinum	
		1/7	NE bronchial dysplasia and adenocarcinoma	
	33[b]	2/33	Small SCLC and metastases in mediastinum	196–350d
		4/33	Small SCLC and lymph vessel invasion	
		1/33	Small SCLC and bronchioalveolar carcinoma	
		1/33	Large SCLC and bronchioalveolar carcinomas	
		14/33	NE hyperplasia, large SCLCS and various metastases	
		6/33	Large SCLCS with independent medullary thyroid carcinomas	
		4/33	Only large SCLCS	
		1/33	Only medullary thyroid carcinomas	

The total number of mice analyzed for each genotype and the occurrence of neuroendocrine and other lung lesions at different time points is presented. Time ranges for sacrifices are indicated in parentheses.

[a] Mice arbitrarily sacrificed.

[b] Mice sacrificed when symptoms occurred or died of age.

$Rb1^{F19/F19}$ mice (Table 1). This is probably due to the long time period required to form primary tumors precluding the formation of metastases. No difference in tumor occurrence or phenotype was found between female and male mice of the same compound genotype.

In a search for further evidence of phenotypic parallels with human SCLC, we evaluated the expression of a variety of epithelial and NE markers. Markers that are positive in human SCLC and that were also detectable in our murine tumors included Syp, neural cell adhesion molecule (Ncam1) (Cavallaro et al., 2001) (Figures 3E, 3F, and 3I), calcitonin-gene related peptide (Cgrp) (Shibayama et al., 2001), and neuron-specific enolase (Kobayashi et al., 1999) (data not shown).

Loss of heterozygosity of both *Rb1* and *Trp53* in murine NE lung tumor formation

The increased median survival of mice with $Trp53^{F2\text{-}10/+};Rb1^{F19/F19}$ and $Trp53^{F2\text{-}10/F2\text{-}10};Rb1^{F19/+}$ genotypes as compared with $Trp53^{F2\text{-}10/F2\text{-}10};Rb1^{F19/F19}$ mice indicates that Rb1 and p53 act synergistically as tumor suppressors for the emergence of murine lung tumors with SCLC phenotype. To further substantiate this finding, we analyzed the MSCLCs from all three genotypes for the loss of *Rb1* and *Trp53* alleles. Southern blot analysis indicated that all primary small cell lung tumors from $Trp53^{F2\text{-}10/F2\text{-}10};Rb1^{F19/F19}$ mice that were analyzed had undergone Cre-mediated deletion of all four conditional alleles (Figure 4A, lanes 4–9). The same holds for the different liver metastases from the individual $Trp53^{F2\text{-}10/F2\text{-}10};Rb1^{F19/F19}$ mice (Figure 4A, lanes 10–13). All (3/5) $Trp53^{F2\text{-}10/+};Rb1^{F19/F19}$ derived tumors that were analyzed had lost the wild-type *Trp53* allele through loss of heterozygosity (Figure 4A, lanes 1–3). Two MSCLC tumors from $Trp53^{F2\text{-}10/F2\text{-}10};Rb1^{F19/+}$ mice that could be analyzed (out of six total) had lost the wild-type *Rb1* allele (Figure 4A, lanes 14 and 15). MSCLCs rapidly proliferated upon subcutaneous grafting in $BalbC^{nu/nu}$ mice. Subsequent analysis of the transplanted tumors more clearly established the loss of both wild-type *Rb1* and *Trp53* alleles that was suggested by the analysis of the primary tumors (Figure 4B). One $Trp53^{F2\text{-}10/F2\text{-}10};Rb1^{F19/+}$ mouse had both adenocarcinomas and MSCLCS. To test whether the floxed *Trp53* and *Rb1* alleles were lost in the morphologically different lesions (Figures 5A and 5B), we performed PCR analysis on DNA extracted from microdissected MSCLC and adenocarcinoma tissue as well as from the adjacent normal lung tissue. We found that in both lesions, both *Trp53* alleles were inactivated. However, in the adenocarcinoma lesion, the wild-type *Rb1* allele was retained, which was in striking contrast to the MSCLC, in which the floxed *Rb1* allele was lost through LOH (Figures 5C and 5D). Similar analyses of two individual single MSCLC lesions in two independent $Trp53^{F2\text{-}10/F2\text{-}10};Rb1^{F19/+}$ mice gave identical results with respect to loss of the wild-type *Rb1* allele (data not shown). These results strongly suggest that p53 inactivation alone is associated with adenocarcinoma phenotype, but that development of MSCLC with its characteristic morphology and neural phenotype is dependent on the inactivation of both *Rb1* and *Trp53*.

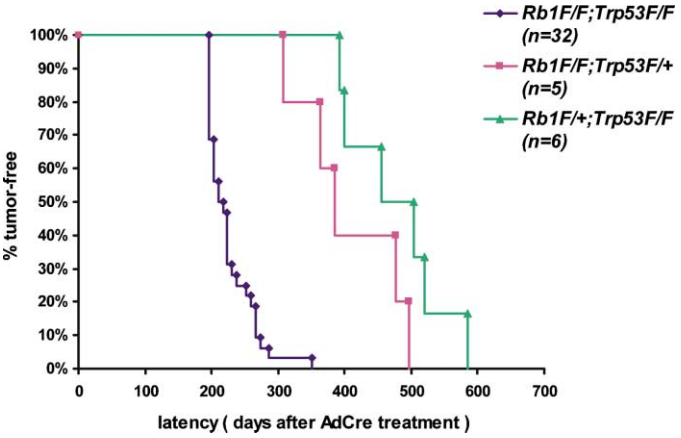

Figure 2. Incidence of NE lung tumors in mice carrying conditional *Rb1* and *Trp53* alleles

Kaplan-Meier lung tumor free mouse survival curve of $Trp53^{F2\text{-}10/F2\text{-}10}$;$Rb1^{F19/F19}$, $Trp53^{F2\text{-}10/+}$;$Rb1^{F19/F19}$, and $Trp53^{F2\text{-}10/F2\text{-}10}$;$Rb1^{F19/+}$ mice. The median time of survival (T_{50}) of the $Trp53^{F2\text{-}10/F2\text{-}10}$;$Rb1^{F19/F19}$ mice is 210 days. For $Trp53^{F2\text{-}10/+}$;$Rb1^{F19/F19}$ and $Trp53^{F2\text{-}10/F2\text{-}10}$;$Rb1^{F19/+}$ mice, T_{50} is 364 and 475 days, respectively. Tumors from each genotype are indicated by different colors. Mice were killed when having severe breathing problems combined with weight loss. All mice had substantial lung tumor load and a subgroup of mice also had primary medullary thyroid carcinomas (see Table 1).

NE differentiation is associated with high *Ascl1* expression

A key marker for human SCLCs is the expression of human achaete-scute complex homolog-like 1 (*ASCL1*) (Borges et al., 1997; Garber et al., 2001; Bhattacharjee et al., 2001). The expression of the murine counterpart of *ASCL1* was only found in clustered pulmonary NE cells or neuroendocrine bodies (NEBs) (Wuenschell et al., 1996; Ito et al., 2000). It has been shown that the expression of this basic helix-loop-helix transcription factor determines the onset and maintenance of NE differentiation in normal pulmonary epithelial cells and also in lung tumors with NE features (Ball et al., 1993; Borges et al., 1997).

Since our primary MSCLCs as well as their metastases were strikingly similar to human SCLC, we immunostained serial sections of the murine lesions for Ascl1 and the NE markers Cgrp and Syp. Morphologically unremarkable NEBs stained very strongly for Cgrp and Syp, while Ascl1 staining was less intense. Ninety percent of focal NE cell proliferations in the lung were positive for Cgrp or synaptophysin (Syp), while 65% were positive for Ascl1 with or without Syp or Cgrp (Figures 6A–6C). Only a small fraction (7%–11%) was exclusively positive for Ascl1 but negative for both other markers. Tumors and hyperplasias stained more intensely for Ascl1 (Figure 7A) than the regular NEBs. Primary tumors (Figures 7A–7D) and liver metastases (Figures 7E–7G) were generally positive for all markers.

Some of the tumors were also positive for Scgb1a1, the Clara cell secretory protein, a marker of the nonciliated secretory (Clara) cells. The liver metastases were all negative for Scgb1a1. These results indicate close resemblance between murine small cell lung tumors and human SCLCs in having high Ascl1 expression activity associated with neural and NE differentiation and maintenance of neuronal markers.

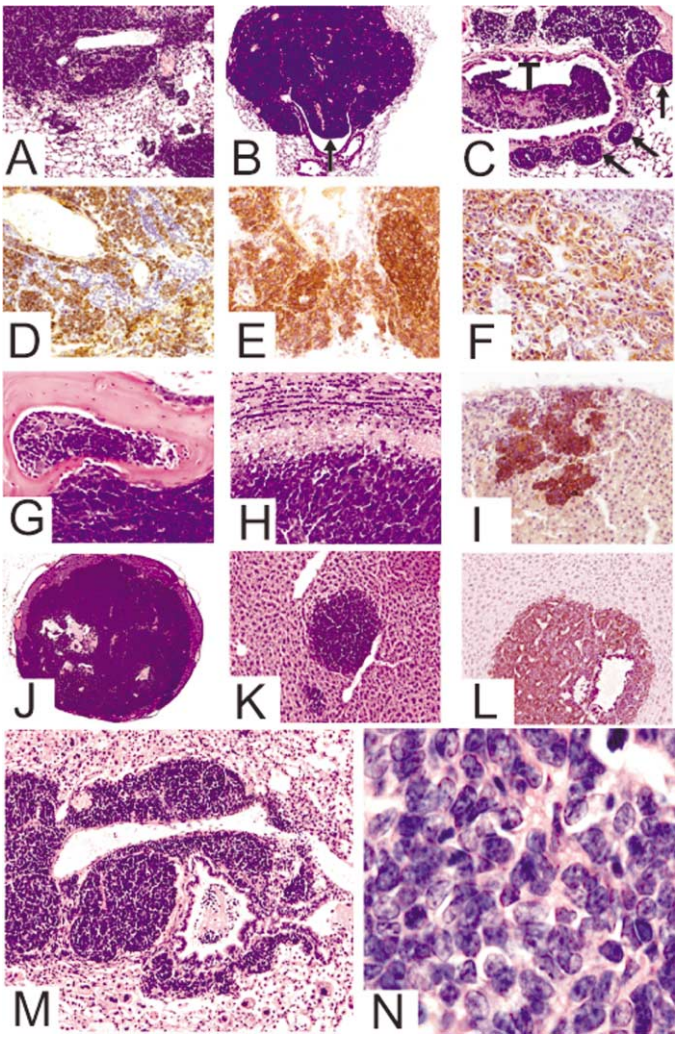

Figure 3. Photomicrographs of NE lung tumors from mice carrying *Trp53* and *Rb1* alleles

Representative lesions are shown from mice after 225–310 days after AdCre treatment.
A: Massive infiltration of lung lobe by MSCLC. Tumors show vascularization and small areas of necrosis and massive infiltration into the surrounding lung parenchyma (H&E staining).
B: Part of the tumor protrudes to bronchiolar lumen (arrow) (H&E staining).
C: Lymphangitic spread (arrows) and an intraluminal component of MSCLC (H&E staining); T = tumor.
D–F: Immunostaining of MSCLC with antisera raised against Titf1 (**D**), Ncam1 (**E**) and Syp (**F**). Infiltrating lymphocytes are negative for Titf1 (**D**).
G–L: MSCLC metastasis into the medullary cavity of the breastbone (**G**). Metastasis into (**H**) forebrain cortex, (**I**) adrenal gland, revealing Syp immunoreactivity and surrounded by negative adrenal cortex, (**J**) ovary, and (**K–L**) liver, with or without immunostaining for Syp.
M: Tumor tissue engulfing and surrounding small airway and adjacent pulmonary blood vessel, without eliciting fibrotic stromal response.
N: High-power field of tumor cells, which feature finely dispersed chromatin. Cytoplasm is scanty and is morphologically featureless, and there is characteristic molding of nuclei of adjacent tumor cells.

Discussion

Since high mutation frequencies of tumor suppressor genes *Rb1* and *Trp53* have been observed in human SCLCs (Minna et al., 2002; Sattler and Salgia, 2003), inactivation of *Rb1* and

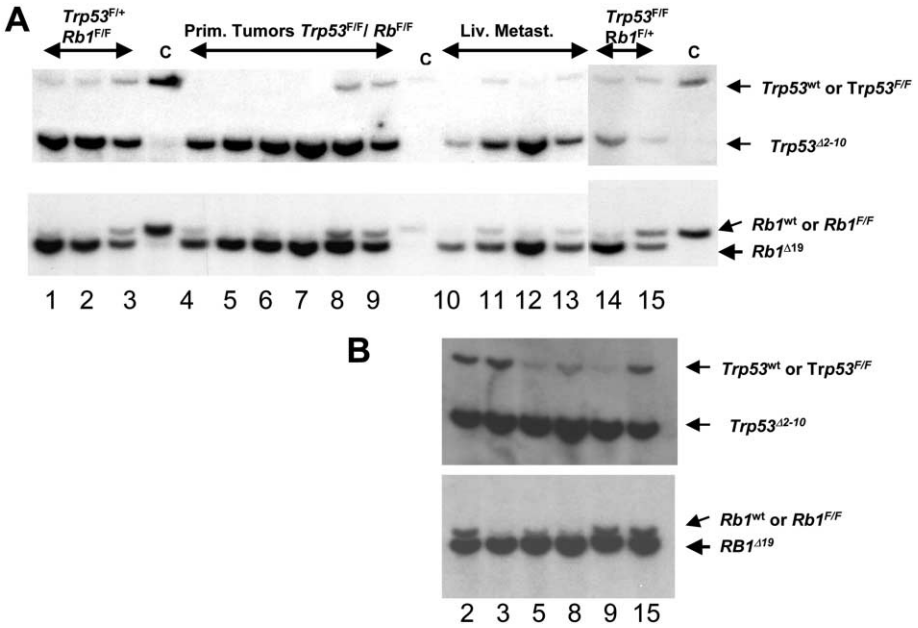

Figure 4. *Trp53* and *Rb1* gene inactivation in NE lung tumors

A: Southern blots of tumor DNA to detect Cre-mediated inactivation of *Trp53* (BglII digestion, *Trp53* XbaI probe) and *Rb1* (PstI digestion, *Rb1* PvuII probe). Representative tumors and control tissues (tail) are shown for each genotype. Numbers under each lane denote individual mice. Arrows indicate the bands corresponding to the different alleles. All NE lung tumors from $Trp53^{F2\text{-}10/F2\text{-}10}$;$Rb1^{F19/F19}$ mice show Cre-mediated deletion of all four conditional alleles. NE lung tumors from $Trp53^{F2\text{-}10/+}$;$Rb1^{F19/F19}$ and $Trp53^{F2\text{-}10/F2\text{-}10}$;$Rb1^{F19/+}$ mice, show in addition to Cre-mediated loss of the floxed *Trp53* and *Rb1* alleles, invariable loss of the wild-type (wt) *Trp53* and Rb1 alleles. In all tumor DNA samples, the remaining hybridization signals are most likely derived from normal contaminating tissue, as indicated by equal intensities of the flox/wt and Δ bands for *Trp53* and *Rb1*, respectively; C = control tail DNA from $Trp53^{F2\text{-}10/F2\text{-}10}$;$Rb1^{F19/F19}$ mice.

B: Samples of primary tumors were transplanted in $Balbc^{nu/nu}$ mice for further tumor propagation with less contamination of normal tissue. Numbers under each lane correspond to the tumors from each individual mouse in **A**. As can be seen, level of contamination is far less and it is very likely that the primary tumors #3 and #15 originally did have LOH for wt *Trp53* and *Rb1* alleles, respectively.

Trp53 seemed a logical approach for establishing a mouse model for SCLC. Introduction of both *Rb1* and *Trp53* lesions into pulmonary epithelial cells via mouse germ line mutations is precluded by the embryonic lethality of *Rb1* null mutants. So far, only mild bronchial and bronchiolar NE cell hyperplasia was found in $Rb1^{+/-}$;$Trp53^{-/-}$ mice (Williams et al., 1994), without progression to a fully malignant phenotype possibly as a result of the strong predisposition to other tumors in the *Trp53*-null background. We therefore decided to use the Cre-*loxP* system for introducing *Rb1* and *Trp53* mutations somatically in a broad range of lung epithelial cells. In a relative short time-span after lung epithelial cells were infected with Ad-Cre virus, we observed small foci of NE cell proliferation in airways, and in these, both alleles of *Rb1* and *Trp53* were inactivated. These lesions progressed to dysplasias and histologically malignant lung tumors, displaying NE differentiation and SCLC morphology. These tumors, which we accordingly designated mouse small cell lung carcinomas (MSCLCs), were highly proliferative, invasive, and had a marked capacity to metastasize to liver, brain, adrenal gland, bone, and ovaries. Taken together, histopathology, immunophenotype, and patterns of growth and dissemination of MSCLC are indeed strikingly similar to human SCLC.

Our data show unambiguously that Rb1 and p53 act synergistically as tumor suppressors in mouse NE tumor formation and that the loss of both *Rb1* and *Trp53* is therefore a prerequisite for NE lung tumor formation. First, Cre-mediated biallelic deletion of *Trp53* and *Rb1* is found in all NE lung tumors from $Trp53^{F2\text{-}10/F2\text{-}10}$;$Rb1^{F19/F19}$ mice. At the same time, however, the focal proliferative lesions could persist as such, since sporadic NE proliferative foci were still detected in mice already having substantial tumor load and even metastases. This might indicate that loss of *Rb1* and *p53* leads to a population of cells that is highly prone to SCLC development but that progression requires additional, more rarely occurring genetic lesions. Alternatively, some of these neoplastic lesions might originate from specific cell types that have limited capacity to progress to overt tumors. Second, NE lung tumors from $Trp53^{F2\text{-}10/+}$;$Rb1^{F19/F19}$ showed LOH of the remaining wild-type allele, and third, $Trp53^{F2\text{-}10/F2\text{-}10}$;$Rb1^{F19/+}$ mice only developed MSCLC upon loss of the wt Rb allele; when the wt Rb allele was retained, adenocarcinomas ensued. Finally, the median latency period of NE lung tumor formation in $Trp53^{F2\text{-}10/F2\text{-}10}$;$Rb1^{F19/F19}$ mice is significantly reduced as compared to $Trp53^{F2\text{-}10/+}$;$Rb1^{F19/F19}$ and $Trp53^{F2\text{-}10/F2\text{-}10}$;$Rb1^{F19/+}$ mice. Single $Trp53^{F2\text{-}10/F2\text{-}10}$ mice yielded only lung adenocarcinomas with similar morphology and tumor latency as seen in $Trp53^{-/-}$ mice (Donehower, 1996). We could not detect any lung tumors in $Rb1^{F19/F19}$ mice up to 18 months after Ad-Cre treatment, nor could we find any hyperproliferative NE cell foci in the airways at earlier time points in these mice. Loss of *Rb1* by itself is therefore insufficient to induce NE neoplasia, and further progression might require the suppression of p53-mediated apoptosis. Interestingly, loss of Rb1 function seems to be crucial in permitting the proliferation of cells expressing the NE differentiation program. Accordingly, no tumors with NE features are found when a functional *Rb1* allele is retained. This is not unexpected, since loss of *Rb1* appears particularly predominant in tumors that derive from neural or NE cells: medulloblastoma, pituitary tumors, retinoblastoma, and PNETs (Marino et al., 2000; Wechsler-Reya and Scott, 2001; Vooijs et al., 1998; Classon and Harlow, 2002; Brodeur, 2003). This is in line with the continued expression of neuronal markers including ASCL1 in the majority of the tumors (Ball et al., 1993). The bHLH transcription factor ASCL1 is expressed both in normal NEBs and in SCLC (Ball et al., 1993; Borges et al., 1997). Repression

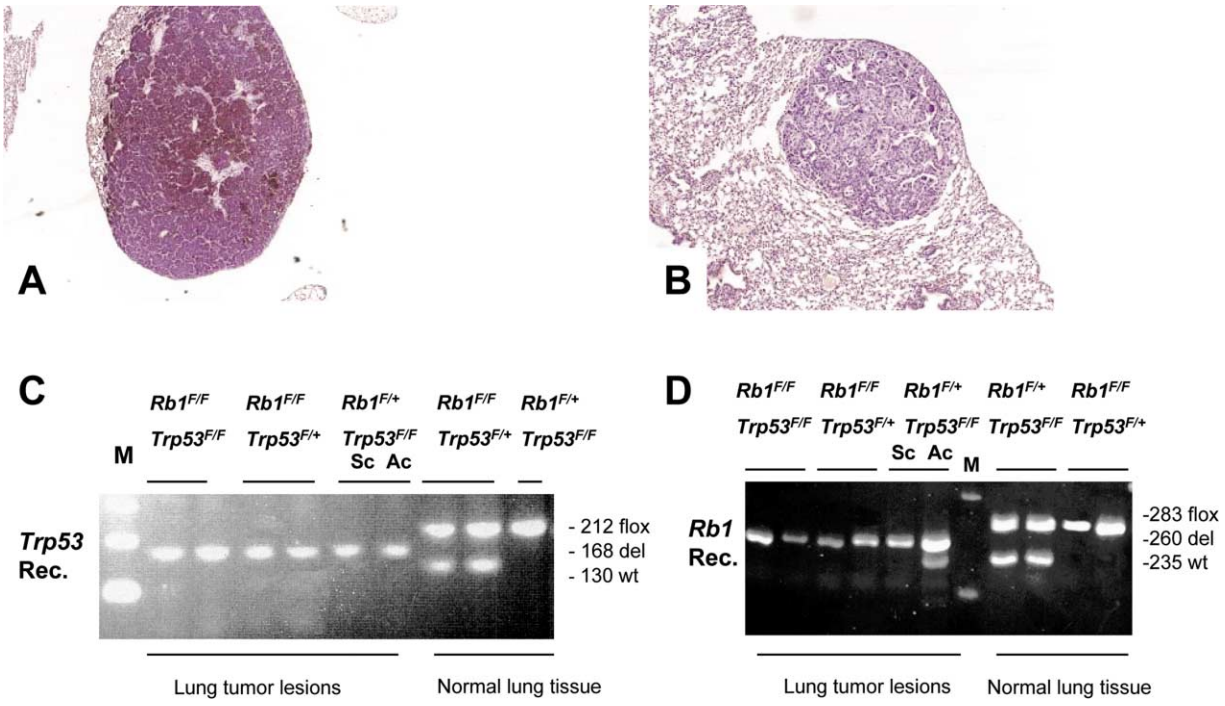

Figure 5. Correlation of histopathology with Cre-mediated *Rb1* and *Trp53* allelic recombination and loss of wt *Rb1* allele in a $Trp53^{F2\text{-}10/F2\text{-}10}/Rb1^{F19/+}$ mouse

A: Immunostaining for the NE marker Syp in MSCLC lesion in part of lung lobe.

B: Lack of immunostaining for Syp in an adenocarcinoma from another lung lobe of the same mouse. Tumor morphologies are markedly different, and only the MSCLC lesion has NE features.

C: PCR-based analysis of *Trp53* and *Rb1* allelic recombination. DNA was isolated from paraffin sections following microdissection of independent tumors from each mouse as indicated. DNA from adjacent normal lung from each mouse served as control tissue. Lanes Sc show PCR fragments using DNA from the MSCLC lesion (**a**), and lanes Ac show PCR products from the adenocarcinoma lesion (**b**), both from identical mouse with indicated genotype, $Trp53^{F2\text{-}10/F2\text{-}10};Rb1^{F19/+}$, above lanes. A 212 bp PCR product represents the floxed, unrecombined $Trp53^{F2\text{-}10}$ alleles, whereas the 168 bp fragment represents a recombined, deleted $Trp53^{F2\text{-}10}$ allele and a 130 bp fragment corresponds to the wt *Trp53* allele. For *Rb1* allelic recombination, a 283-, 260-, and 235-bp product corresponds to the floxed, the recombined, and wt *Rb1* allele, respectively. DNA fragments for *Trp53* recombination show only the 168 bp fragment, meaning that in the control tumors as well as lesion (**a** and **b**), all *Trp53* alleles are inactivated. For the DNA fragments corresponding to *Rb1* recombination, this holds true for all the control tumor lesions and the small cell tumor lesion (**a**). The adenocarcinomas lesion, however, still has a wt *Rb1* allele retained producing a 235 bp fragment.

of *ASCL1* leads to loss of NE differentiation in human SCLC cultures (Borges et al., 1997), underlining its pivotal role in establishment and maintenance of the NE differentiation phenotype. The expression pattern of *Ascl1* in early NE hyperplasia and in primary NE lung tumors in our mutants suggests that $Rb1^{\Delta 19;Trp53\Delta 2\text{-}10}$ tumors originated from progenitors of pulmonary NE cells. However, since not all neural tumors express this marker, it is more probable that it serves as a marker of cell of origin or lineage than that its expression is directly or indirectly regulated by Rb1, even though Rb1 may be involved in modulating the expression of a suppressor of *Ascl11*, *Hes1* (Lasorella et al., 2000; Jogi et al., 2002; Toma et al., 2000). Previous studies showed that somatic activation of *Kras2* in the same pulmonary epithelial target cells generates only pulmonary adenocarcinomas (Meuwissen et al., 2001; Jackson et al., 2001). Thus, two morphologically distinct tumor types result from the different genetic lesions that are introduced. Most likely, identical lesions exhibit strong cell type-dependent effects, leading to transformation of divergent target cells. For instance, *Kras2* would then have a profound different effect in pulmonary NE cells as compared to alveolar type II cells. Alternatively, different lesions might drive the same target cells into a dissimilar path of differentiation. In favor of the latter possibility is the observation that in CGRP-*Hras* mice, expression of Hras in pulmonary NE epithelial cells caused only bronchial adenocarcinomas, even though CGRP-*Hras* lost its activity in fully developed adenocarcinomas. This suggests an active repression of neuronal differentiation in the original NE target cells by an active Ras pathway (Sunday et al., 1999). In contrast, the loss of both *Rb1* and *Trp53* seems to impose or allow for the maintenance of NE differentiation and proliferation.

Considering the variety of markers that are expressed in our MSCLC, we favor a model in which different progenitors of the NE lineage can serve as cells of origin for SCLC. Some of these progenitors might also serve as precursors of Clara cells. Indeed, there is evidence that injured or depleted Clara cells can be replaced from common precursors for both Clara and NE cells (Reynolds et al., 2000a, 2000b). This pool of precursor cells might be widely present throughout the airway epithelium and thus serve as a plausible target for Ad-Cre virus infection. Primary NE tumors derived from these common precursor cells could then partially retain SCGB1A1 expression, as we observed. This also argues for an earlier progenitor or lung epithelial stem cell being the target cell that gives rise to MSCLC. A recent study provided further support for this by showing that a similar pattern of sonic hedgehog (SHH) signaling observed

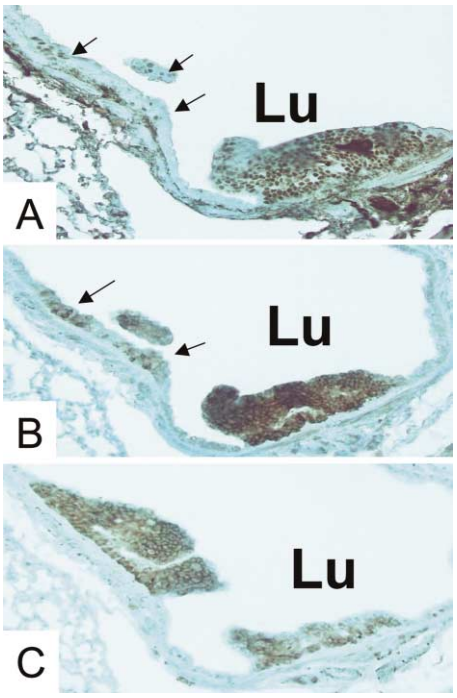

Figure 6. Pulmonary NE cell hyperplasia

Serial sections were obtained from a *Trp53*$^{F2\text{-}10/F2\text{-}10}$;*Rb1*$^{F19/F19}$ mouse, 11 weeks after Ad-Cre treatment.
A: Hyperplastic lesions reveal strong nuclear staining for Ascl1, while most of the epithelium lining the bronchial lumen is negative. Scattered cells express Ascl1 (arrows).
B: Cytoplasmic Cgrp immunostaining in scattered epithelial cells (arrows) and in the larger lesion on the right.
C: Two large areas of Syp-positive hyperplasias of the epithelium. Lu = lumen.

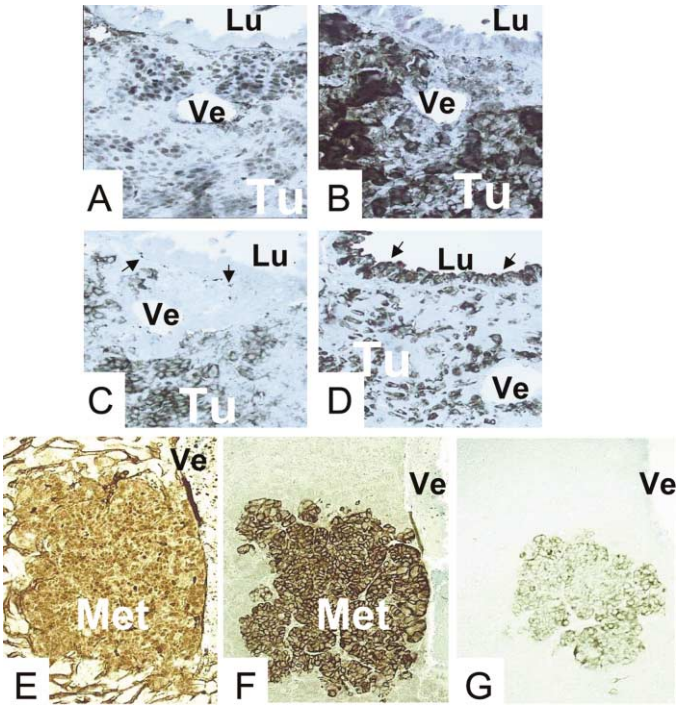

Figure 7. NE differentiation in primary and metastatic MSCLC

Serial sections were obtained from a *Trp53*$^{F2\text{-}10/F2\text{-}10}$;*Rb1*$^{F19/F19}$ mouse, 36 weeks after Ad-Cre treatment.
A: A primary MSCLC reveals strong nuclear immunostaining for Ascl1, while the epithelium lining the airway lumen is negative.
B: The same tumor is strongly positive for anti-Cgrp staining which shows a cytoplasmic pattern. The airway epithelium remains negative.
C: Positive immunostaining for Syp, also with a cytoplasmic pattern. A few positive nerve fibers can be seen below the unstained epithelium (arrows).
D: Airway epithelium is strongly positive for Scgb1a1 (arrows) together with scattered tumor cells. Bronchiolar lumen (Lu), vessel (Ve), and tumor (Tu).
E: Anti-Ascl1 staining showing nuclear positivity in a liver metastasis from the same mouse, surrounded by parenchyma revealing lace-like planes of unstained liver cells.
F: The same lesion was positive for Cgrp, whereas liver cells remained negative.
G: Anti-Syp staining surrounded by negative liver cells. Metastasis (Met) and vessel (Ve).

in NE precursor cells was also found in a subset of human SCLCs and that an active SHH pathway is crucial in maintaining proliferation and NE differentiation in SCLC (Watkins et al., 2003).

The early NE progenitor cells would only require loss of *Rb1* to secure proliferation of this particular cell type without the need for additional loss of *p130* or *p107* function. In contrast, the functional redundancy of all three pocket proteins (Lipinski and Jacks, 1999; Dannenberg et al., 2000; Sage et al., 2000) is probably effective in non-NE pulmonary epithelial cells along the airways, thus explaining the massive adenocarcinomas seen in *CC10-SV40Tag* (Magdaleno et al., 1997; Linnoila et al., 2000) and their almost complete absence in *Trp53*$^{F2\text{-}10/F2\text{-}10}$;*Rb1*$^{F19/F19}$ mice.

The model presented in this study shows that somatic inactivation of both *Rb1* and *Trp53* alleles in lung epithelial cells readily leads to formation of small cell NE tumors. Since their histopathologic characteristics and metastasizing capacity are strikingly similar to human SCLCs, we have termed them MSCLC. Our model may prove a valuable tool for (1) comparing genotype-phenotype similarities between human SCLC and MSCLC, (2) the identification of precursor lesions and (3) additional factors involved in tumor progression, and (4) ultimately, testing of targeted, novel tumor intervention strategies and chemoprevention.

Experimental procedures

Intratracheal Adeno-Cre virus administration

One series of mice was infected with Ad-Cre virus by an injection into the trachea as described in previous study (Meuwissen et al., 2001), whereas another series was intratracheally intubated.

Genotyping of mice

We detected the *Trp53*$^{F2\text{-}10}$ allele by PCR amplification of the *loxP* site in intron 10, yielding products of 584 bp and 431 bp for the floxed and wild-type alleles using primers p53-10F (5′- AAGGGGTATGAGGGACAAGG-3′) and p53-10R (5′-GAAGACAGAAAAGGGGAGGG-3′). Detection of the *Trp53*$^{\Delta2\text{-}10}$ allele yielded a 612 bp fragment using primers p53-10F and p53-10R. The *Rb1*^{F19} allele was detected using primers Rb18 (5′-GGCGTGTGCCA TCAAT-3′) and Rb19 (5′-AACTCAAGGGAGACCTG-3′) yielding products of 650 and 490 bp for the floxed and wild-type alleles, respectively. For all PCR reactions, thermocyling conditions consisted of 30 cycles of 30 s at 95°C, 30 s at 58°C, and 50 s at 72°C. Reactions contain approximately 200 ng of template DNA, 0.5 μM primers, 100 μM dNTPs, 2.5 U of *Taq* DNA polymerase, 2.5 mM MgCl2, and 1× PCR buffer in a 25 μl volume.

DNA analysis

We isolated high molecular weight DNA from tail or other mouse tissues as described (Laird et al., 1991). We carried out Southern blot analysis with 10 μg of genomic DNA digested with the appropriate restriction enzymes. Blotting and hybridization were performed as described (Jonkers et al., 2001). The probes corresponding to *Rb1* exon 19 and *Trp53* exon 11 were labeled by PCR. We isolated the *Trp53* 5′ XbaI probe as a 700 nt genomic XbaI fragment, subcloned it in PBSK and labeled it by PCR.

The *Rb1* fragment from exon 19 was subcloned and oligo-labeled as described (Vooijs et al., 1998).

PCR analysis of recombination

Microdissection of tumors and of adjacent normal lung tumor tissue was performed using a laser capture microdissection system (Arcturus). Five μm sections from formalin-fixed paraffin-embedded material were used after dewaxing in xylene and drying. The dissected material was transferred into 50 μl of proteinase K buffer and incubated at 56°C overnight, after which the proteinase K buffer was inactivated for 10 min at 95°C.

Two microliters were used for subsequent PCR amplification using primers Rb212 (5′- GAAAGGAAAGTCAGGGACATTGGG-3′), Rb18 (5′-GGCGTG TGCCATCAATG-3′), and Rb19E (5′-CTCAAGAGCTCAGACTCATGG-3′) yielding a 283 bp product for the unrecombined $Rb1^{F19}$ allele (primers Rb19E and Rb18), a 260 bp product for the recombined $Rb1^{\Delta 19}$ allele (primers Rb212 and Rb18), and a 235 bp fragment for the wild-type *Rb1* allele (primers Rb19E and Rb18, smaller fragment contains no LoxP sequences) as described in Vooijs et al., (1998) and Marino et al., 2000). *Trp53* allelic recombination makes use of a three-primer set: P53-1, P53-2, and P53-3. Primers P53-1 (5′-CGCAATCCTTTATTCTGTTCG-3′) and P53-2 (5′-AGCACATAGGAGGC AGAGAC-3′) are flanking the first Lox P site, and primer P53-3 (5′-TGAGACA GGGTCTTGCTATTG-3′) is located downstream of the 3′ Lox P site in the conditional $Trp53^{F2\text{-}10}$ allele. For detecting $Trp53^{F2\text{-}11}$ allele recombination, PCR products yield a 212 bp fragment for the floxed, unrecombined $Trp53^{F2\text{-}11}$ allele (primers P53-1 and P53-2), a 168 bp fragment for the recombined or deleted $Trp53^{\Delta 2\text{-}10}$ allele (primers P53-1 and P53-3), and a 130 bp for the wild-type *Trp53* allele (primers P53-1 and P53-2, wt fragment is shorter due to the lack of Lox P sequences). The thermocycling conditions for all PCR reactions consisted of 39 cycles of 30 s at 94°C, 35 s at 58°C, and 50 s at 72°C. The PCR mix consisted of 0.5 μM primers, 100 μM dNTPs, 9% glycerol, and 2.5 units of *Taq* polymerase in a 20 μl volume. A hot start was provided using Invitrogen hot-wax MgCl2 beads (1.5 mM). PCR products were analyzed on a 3% NuSieve agarose gel.

Tissue preparation and histological analysis

Mouse tissues for histopathology were fixed in 4% PFA-PBS for at least 48 hr. Lungs were first separately inflated with syringe through trachea with 4% PFA-PBS. Fixed tissues were dehydrated, embedded in Histowax, cut into 5 μm sections, and stained with hematoxylin and eosin (H&E) stain. We carried out immunohistochemistry for Titf1 (monoclonal, 1:40,000, Dako), Ncam1 (polyclonal, 1:200, Chemicon), syp (polyclonal, 1:100, Zymed), Ascl1 (monoclonal, 1:50, BD Bioscience/Pharmingen), CC-10 (polyclonal, 1:10,000), Cgrp (polyclonal, 1:3,000, Sigma), and Brdu (1:50, Dako) using biotinylated secondary antibodies (goat anti-rabbit, 1:800 and goat anti-mouse, 1:600; Dako). For visualization, we used streptavidin-peroxidase (Dako or Vectastain) and diaminobenzidine as a chromogen.

Acknowledgments

We thank L. Rijswijk and F. van de Ahé for expert assistance with the microsurgical procedures, J. Bulthuis, K. de Goeij, M. Tjin-a-Koeng, and Xu Naizhen for histotechnical assistance, N. Bosnie and A. Zwerver for animal care, and F. DeMayo for providing us with anti-CC10 antibody. S.C.L. was a recipient of a Dutch Cancer Society research fellowship. This work was supported by a grant of the Dutch Cancer Society (R.M.).

Received: July 7, 2003
Revised: August 22, 2003
Published: September 22, 2003

References

Ball, D.W., Azzoli, C.G., Baylin, S.B., Chi, D., Dou, S., Donis-Keller, H., Cumaraswamy, A., Borges, M., and Nelkin, B.D. (1993). Identification of a human achaete-scute homolog highly expressed in neuroendocrine tumors. Proc. Natl. Acad. Sci. USA *90*, 5648–5652.

Bhattacharjee, A., Richards, W.G., Staunton, J., Li, C., Monti, S., Vasa, P., Ladd, C., Beheshti, J., Bueno, R., Gillette, M., et al. (2001). Classification of human lung carcinomas by mRNA expression profiling reveals distinct adenocarcinoma subclasses. Proc. Natl. Acad. Sci. USA *98*, 13790–13795.

Borges, M., Linnoila, R.I., van de Velde, H.J., Chen, H., Nelkin, B.D., Mabry, M., Baylin, S.B., and Ball, D.W. (1997). An achaete-scute homologue essential for neuroendocrine differentiation in the lung. Nature *386*, 852–855.

Brodeur, G.M. (2003). Neuroblastoma: biological insights into a clinical enigma. Nat. Rev. Cancer *3*, 203–216.

Cavallaro, U., Niedermeyer, J., Fuxa, M., and Christofori, G. (2001). N-CAM modulates tumour-cell adhesion to matrix by inducing FGF-receptor signalling. Nat. Cell Biol. *3*, 650–657.

Classon, M., and Harlow, E. (2002). The retinoblastoma tumour suppressor in development and cancer. Nat. Rev. Cancer *2*, 910–917.

Dannenberg, J.H., van Rossum, A., Schuijff, L., and te Riele, H. (2000). Ablation of the retinoblastoma gene family deregulates G(1) control causing immortalization and increased cell turnover under growth-restricting conditions. Genes Dev. *14*, 3051–3064.

Donehower, L.A. (1996). The p53-deficient mouse: a model for basic and applied cancer studies. Semin. Cancer Biol. *7*, 269–278.

Ferrari, L., Seregni, E., Bajetta, E., Martinetti, A., and Bombardieri, E. (1999). The biological characteristics of chromogranin A and its role as a circulating marker in neuroendocrine tumours. Anticancer Res. *19*, 3415–3427.

Garber, M.E., Troyanskaya, O.G., Schluens, K., Petersen, S., Thaesler, Z., Pacyna-Gengelbach, M., van de Rijn, M., Rosen, G.D., Perou, C.M., Whyte, R.I., et al. (2001). Diversity of gene expression in adenocarcinoma of the lung. Proc. Natl. Acad. Sci. USA *98*, 13784–13789.

Gouyer, V., Gazzeri, S., Bolon, I., Drevet, C., Brambilla, C., and Brambilla, E. (1998). Mechanism of retinoblastoma gene inactivation in the spectrum of neuroendocrine lung tumors. Am. J. Respir. Cell Mol. Biol. *18*, 188–196.

Ito, T., Udaka, N., Yazawa, T., Okudela, K., Hayashi, H., Sudo, T., Guillemot, F., Kageyama, R., and Kitamura, H. (2000). Basic helix-loop-helix transcription factors regulate the neuroendocrine differentiation of fetal mouse pulmonary epithelium. Development *127*, 3913–3921.

Jacks, T., Fazeli, A., Schmitt, E.M., Bronson, R.T., Goodell, M.A., and Weinberg, R.A. (1992). Effects of an Rb mutation in the mouse. Nature *359*, 295–300.

Jackson, E.L., Willis, N., Mercer, K., Bronson, R.T., Crowley, D., Montoya, R., Jacks, T., and Tuveson, D.A. (2001). Analysis of lung tumor initiation and progression using conditional expression of oncogenic K-ras. Genes Dev. *15*, 3243–3248.

Jogi, A., Persson, P., Grynfeld, A., Pahlman, S., and Axelson, H. (2002). Modulation of basic helix-loop-helix transcription complex formation by Id proteins during neuronal differentiation. J. Biol. Chem. *277*, 9118–9126.

Jonkers, J., Meuwissen, R., van der Gulden, H., Peterse, H., van der Valk, M., and Berns, A. (2001). Synergistic tumor suppressor activity of BRCA2 and p53 in a conditional mouse model for breast cancer. Nat. Genet. *29*, 418–425.

Junker, K., Wiethege, T., and Muller, K.M. (2000). Pathology of small-cell lung cancer. J. Cancer Res. Clin. Oncol. *126*, 361–368.

Kobayashi, S., Okada, S., Hasumi, T., Sato, N., and Fujimura, S. (1999). The significance of NSE and CEA as a diffrentiation marker for the cellular heterogeneity of small cell lung cancer. Tohoku J. Exp. Med. *189*, 37–49.

Laird, P.W., Zijderveld, A., Linders, K., Rudnicki, M.A., Jaenisch, R., and Berns, A. (1991). Simplified mammalian DNA isolation procedure. Nucleic Acids Res. *19*, 4293.

Lasorella, A., Noseda, M., Beyna, M., Yokota, Y., and Iavarone, A. (2000). Id2 is a retinoblastoma protein target and mediates signalling by Myc oncoproteins. Nature *407*, 592–598.

Linnoila, R.I., Zhao, B., DeMayo, J.L., Nelkin, B.D., Baylin, S.B., DeMayo, F.J., and Ball, D.W. (2000). Constitutive achaete-scute homologue-1 promotes airway dysplasia and lung neuroendocrine tumors in transgenic mice. Cancer Res. *60*, 4005–4009.

Lipinski, M.M., and Jacks, T. (1999). The retinoblastoma gene family in differentiation and development. Oncogene *18*, 7873–7882.

Maandag, E.C., van der Valk, M., Vlaar, M., Feltkamp, C., O'Brien, J., van Roon, M., van der Lugt, N., Berns, A., and te Riele, H. (1994). Developmental rescue of an embryonic-lethal mutation in the retinoblastoma gene in chimeric mice. EMBO J. *13*, 4260–4268.

Magdaleno, S.M., Wang, G., Mireles, V.L., Ray, M.K., Finegold, M.J., and DeMayo, F.J. (1997). Cyclin-dependent kinase inhibitor expression in pulmonary Clara cells transformed with SV40 large T antigen in transgenic mice. Cell Growth Differ. *8*, 145–155.

Marino, S., Vooijs, M., van Der Gulden, H., Jonkers, J., and Berns, A. (2000). Induction of medulloblastomas in p53-null mutant mice by somatic inactivation of Rb in the external granular layer cells of the cerebellum. Genes Dev. *14*, 994–1004.

Meuwissen, R., Linn, S.C., van der Valk, M., Mooi, W.J., and Berns, A. (2001). Mouse model for lung tumorigenesis through Cre/lox controlled sporadic activation of the K-Ras oncogene. Oncogene *20*, 6551–6558.

Minna, J.D., Roth, J.A., and Gazdar, A.F. (2002). Focus on lung cancer. Cancer Cell *1*, 49–52.

Ordonez, N.G. (2000). Value of thyroid transcription factor-1 immunostaining in distinguishing small cell lung carcinomas from other small cell carcinomas. Am. J. Surg. Pathol. *24*, 1217–1223.

Reynolds, S.D., Giangreco, A., Power, J.H., and Stripp, B.R. (2000a). Neuroepithelial bodies of pulmonary airways serve as a reservoir of progenitor cells capable of epithelial regeneration. Am. J. Pathol. *156*, 269–278.

Reynolds, S.D., Hong, K.U., Giangreco, A., Mango, G.W., Guron, C., Morimoto, Y., and Stripp, B.R. (2000b). Conditional clara cell ablation reveals a self-renewing progenitor function of pulmonary neuroendocrine cells. Am. J. Physiol. Lung Cell. Mol. Physiol. *278*, L1256–L1263.

Rom, W.N., Hay, J.G., Lee, T.C., Jiang, Y., and Tchou-Wong, K.M. (2000). Molecular and genetic aspects of lung cancer. Am. J. Respir. Crit. Care Med. *161*, 1355–1367.

Sage, J., Mulligan, G.J., Attardi, L.D., Miller, A., Chen, S., Williams, B., Theodorou, E., and Jacks, T. (2000). Targeted disruption of the three Rb-related genes leads to loss of G(1) control and immortalization. Genes Dev. *14*, 3037–3050.

Sandler, A.B. (2003). Chemotherapy for small cell lung cancer. Semin. Oncol. *30*, 9–25.

Sattler, M., and Salgia, R. (2003). Molecular and cellular biology of small cell lung cancer. Semin. Oncol. *30*, 57–71.

Sekido, Y., Fong, K.M., and Minna, J.D. (2003). Molecular genetics of lung cancer. Annu. Rev. Med. *54*, 73–87.

Sherr, C.J., and McCormick, F. (2002). The RB and p53 pathways in cancer. Cancer Cell *2*, 103–112.

Shibayama, T., Ueoka, H., Nishii, K., Kiura, K., Tabata, M., Miyatake, K., Kitajima, T., and Harada, M. (2001). Complementary roles of pro-gastrin-releasing peptide (ProGRP) and neuron specific enolase (NSE) in diagnosis and prognosis of small-cell lung cancer (SCLC). Lung Cancer *32*, 61–69.

Sunday, M.E., Haley, K.J., Sikorski, K., Graham, S.A., Emanuel, R.L., Zhang, F., Mu, Q., Shahsafaei, A., and Hatzis, D. (1999). Calcitonin driven v-Ha-ras induces multilineage pulmonary epithelial hyperplasias and neoplasms. Oncogene *18*, 4336–4347.

Toma, J.G., El Bizri, H., Barnabe-Heider, F., Aloyz, R., and Miller, F.D. (2000). Evidence that helix-loop-helix proteins collaborate with retinoblastoma tumor suppressor protein to regulate cortical neurogenesis. J. Neurosci. *20*, 7648–7656.

Tyczynski, J.E., Bray, F., and Parkin, D.M. (2003). Lung cancer in Europe in 2000: epidemiology, prevention, and early detection. Lancet Oncol. *4*, 45–55.

Vooijs, M., van der Valk, M., te Riele, H., and Berns, A. (1998). Flp-mediated tissue-specific inactivation of the retinoblastoma tumor suppressor gene in the mouse. Oncogene *17*, 1–12.

Watkins, D.N., Berman, D.M., Burkholder, S.G., Wang, B., Beachy, P.A., and Baylin, S.B. (2003). Hedgehog signalling within airway epithelial progenitors and in small-cell lung cancer. Nature *422*, 313–317.

Wechsler-Reya, R., and Scott, M.P. (2001). The developmental biology of brain tumors. Annu. Rev. Neurosci. *24*, 385–428.

Williams, B.O., Remington, L., Albert, D.M., Mukai, S., Bronson, R.T., and Jacks, T. (1994). Cooperative tumorigenic effects of germline mutations in Rb and p53. Nat. Genet. *7*, 480–484.

Wistuba, I.I., Gazdar, A.F., and Minna, J.D. (2001). Molecular genetics of small cell lung carcinoma. Semin. Oncol. *28*, 3–13.

Wu, M., Wang, B., Gil, J., Sabo, E., Miller, L., Gan, L., and Burstein, D.E. (2003). p63 and TTF-1 immunostaining. A useful marker panel for distinguishing small cell carcinoma of lung from poorly differentiated squamous cell carcinoma of lung. Am. J. Clin. Pathol. *119*, 696–702.

Wuenschell, C.W., Sunday, M.E., Singh, G., Minoo, P., Slavkin, H.C., and Warburton, D. (1996). Embryonic mouse lung epithelial progenitor cells coexpress immunohistochemical markers of diverse mature cell lineages. J. Histochem. Cytochem. *44*, 113–123.